Review | Received 7 May 2025; Revised 17 July 2025; Accepted 7 August 2025; Published 21 August 2025
https://doi.org/10.55092/aimat20250012

Machine learning in research and development of advanced nuclear materials: a systematic review for continuum-scale modelling

Chaoyue Jin and Shurong Ding*

Institute of Mechanics and Computational Engineering, Department of Aeronautics and Astronautics, Fudan University, Shanghai 200433, China

* Correspondence author; E-mail: dingshurong@fudan.edu.cn.

Highlights:

- Comprehensive review of machine learning applications in nuclear materials research, covering microstructural analysis, thermal conductivity prediction, and mechanical behavior modeling.
- Identification of key challenges including irradiation-induced thermo-mechanical coupling, feature selection for physically meaningful inputs, and scarcity of high-quality datasets.
- This review highlights future research directions that emphasize hybrid ML–physics frameworks, time-dependent modeling with temporal–spatial correlations, and physics-informed dataset generation via finite element simulations.

Abstract: Advanced nuclear materials should be developed to support the new-type nuclear reactors with high economy and high safety. The nuclear materials refer to the nuclear fuels and nuclear structural materials, needing to have excellent thermo-mechanical performances under the extreme in-pile neutron-irradiation conditions. Their irradiation-induced thermo-mechanical properties are dynamically varying and generally related to the temperatures, the irradiation doses, the chemical components and the as-fabricated microstructures depending on the manufacture process parameters, posing significant challenges to their accurate modeling and precise prediction across all relevant length- and time-scales. It is widely acknowledged that characterizing and understanding these properties and behaviors demands abundant irradiation data; however, such experiments are very expensive and time-consuming. Consequently, multi-scale theoretical modeling and numerical simulations have been widely employed and are frequently reported in the literatures. Recent advances in machine learning (ML) now offer powerful, data-driven strategies to accelerate these efforts, enabling rapid property prediction, composition and fabrication-process optimization for advanced materials. This review begins by introducing the critical thermo-mechanical responses of nuclear fuels and structural materials under irradiation. Subsequently, current continuum-scale applications of ML in the research and development of advanced nuclear materials are investigated and discussed. Simultaneously, the prospects and limitations of ML in this field are evaluated. It is pointed out that ML should be combined with the advanced modeling and numerical simulation, and it is particularly important to

enhance the understanding of the physical problems, select appropriate AI algorithms and incorporate necessary physical constraints with strong generalization capabilities.

Keywords: nuclear materials; machine learning; nuclear fuels; nuclear cladding; thermo-mechanical properties; irradiation-induced thermo-mechanical coupling behaviors

1. Introduction

Nuclear energy is widely regarded as a crucial clean energy source, renowned for its efficiency and stability [1,2]. Since the mid-20th century, nuclear energy has become a cornerstone of many national energy strategies [3], playing an integral role in mitigating climate change and reducing carbon emissions [4]. In addition to electricity generation, nuclear engineering finds extensive applications in medicine, industry, and agriculture [5]. Nonetheless, the application of nuclear energy presents significant challenges, especially concerning safety and material performance. Accidents like those at Chernobyl, Fukushima, and Three Mile Island have amplified public concerns about nuclear safety [6].

The operating environment within nuclear reactors is exceptionally harsh, characterized by high temperatures, elevated pressure, intense irradiation, and chemical corrosion [7,8]. Under these conditions, material failure can lead to serious consequences, compromising the safe operation of the reactor. As a result, the nuclear industry imposes exceptionally stringent standards on materials, requiring them to maintain stable physical and chemical properties over prolonged periods in extreme environments.

Nuclear materials are generally classified into two categories: nuclear fuels and structural materials. Nuclear fuels typically consist of uranium- or plutonium-based oxides or metal compounds, which must undergo fission reactions efficiently under high temperatures and neutron irradiation. Common nuclear fuels, including UMo alloys [9] and UO_2 [10], have been extensively studied over the past decades. However, challenges persist regarding the loss of geometric stability in fuel element structures, caused by irradiation-induced swelling and creep deformation. Structural materials serve as protective layers surrounding the nuclear fuel, primarily preventing the leakage of radioactive fission products into the reactor coolant. Zr alloys are widely used as cladding materials [11]. However, their severe hydrogen embrittlement remains an instability factor that threatens reactor safety [12]. Structural materials must exhibit excellent mechanical strength, corrosion resistance, and irradiation tolerance under extreme conditions. The coupled thermo-mechanical responses caused by irradiation in reactor-core nuclear components are critical to the optimal design of advanced nuclear systems.

To support the development of advanced nuclear reactors characterized by high economic efficiency and enhanced safety, researchers continually conduct experiments aimed at improving material performances. These experiments encompass the material synthesis, processing, characterization, and performance evaluation. Through experimental investigations, researchers explore elemental doping and process optimization to enhance material stability and longevity [13–15].

Experimental studies for nuclear materials present considerable challenges. On one hand, the experimental procedures are complex, requiring precise equipment and stringent safety protocols [16]. On the other hand, testing nuclear materials entails long experimental cycles and high costs [5]. For instance, irradiation damage experiments require extended high-irradiation simulations, while high-temperature, high-pressure tests demand specialized setups. The high experimental costs and lengthy cycles hinder the development of new materials, impeding the ability to rapidly meet the evolving demands

of the nuclear industry.

Computational technology has played a fundamental role in driving advancements in the nuclear field. Reactor simulation software based on high-performance computing encompasses domains such as neutronics, heat transfer, fuel behavior, transient analysis, and mechanics, providing crucial tools and data for reactor research, development, and safety evaluations [17–19]. In recent years, machine learning (ML), a key branch of artificial intelligence, has seen rapid advancements. ML algorithms, including supervised learning, unsupervised learning, and reinforcement learning, are capable of automatically extracting patterns and rules from large datasets to make predictions and decisions. These algorithms have demonstrated significant success in image recognition, speech recognition, and natural language processing [20–23].

The rapid advancement of ML has created new opportunities for materials science. ML algorithms can efficiently extract valuable information from extensive experimental and literature data to predict material properties and behaviors. For instance, ML-based materials design can accelerate the discovery of novel materials, optimize compositions and structures, and improve performance [24]. In materials science, ML has been applied to alloy design, catalyst development, and polymer research, yielding substantial outcomes [25–29]. Current numerical simulation techniques are highly advanced, with simulation results closely matching experimental observations. Consequently, large-scale numerical simulations are widely used to develop surrogate models for databases, effectively replacing experimental costs with computational expenditures [30–32]. Additionally, transfer learning techniques are extensively employed to mitigate reliability challenges in training models with limited datasets [33–36].

The nuclear field has also begun to extensively apply ML techniques to address complex issues in material property prediction and optimization. For instance, ML models can predict the behavior of nuclear fuels under various conditions and optimize the composition and processing techniques of cladding materials [37–41]. Moreover, ML is employed for fault diagnosis and safety assessment in nuclear reactors, which improves operational reliability and efficiency in nuclear power generation [42,43]. The integration of ML has significantly increased the efficiency of nuclear material research and development, while substantially reducing experimental costs and durations.

This review examines the application of ML in the development of nuclear fuel and structural materials. First, the important thermo-mechanical properties and behaviors of nuclear materials under irradiation are introduced, together with the existing experimental studies, theoretical modeling and numerical simulation research. Then, the current applications of ML in the research and development of advanced nuclear materials are presented in detail. Finally, the prospects and limitations of ML are discussed. It is emphasized that ML should be integrated with advanced modeling and numerical simulations, due to the insufficient experimental data available during and after irradiation. It is important to clarify that this review focuses on the application of various ML models, rather than providing a detailed explanation of their underlying algorithms. References to the ML algorithms discussed in this study are provided for readers interested in further investigation. Additionally, this review is restricted to continuum-scale frameworks, excluding atomic-level approaches such as density functional theory (DFT) and molecular dynamics (MD).

2. Thermo-mechanical responses of nuclear materials under irradiation

The thermo-mechanical responses of materials under irradiation evolve dynamically and are predominantly governed by the combined effects of temperature and irradiation dose. Within such environments, nuclear fuels and structural materials undergo a range of irradiation-driven phenomena, including hardening, embrittlement, creep and volumetric swelling.

2.1. Nuclear fuel

2.1.1. Fission solid swelling

In nuclear fuels, swelling caused by the accumulation of both solid and gas fission products manifests as a macroscopic volume increase. This deformation represents a critical concern in the design of nuclear reactor cores [44]. Kim and Hofman [45] proposed an empirical formula for fission solid swelling of UMo alloys, establishing a linear relationship between solid fission swelling and fission density, expressed as

$$SW_{solid} = 4.0F_d \quad (1)$$

where SW_{solid} denotes the volume strain caused by fission solid products in %; F_{d} is fission density in 10^{27}fission/m^3. Suzuki and Saitou [46] also developed a linear model for UO_2 fission solid swelling:

$$SW_{solid} = 2.5F_d \quad (2)$$

2.1.2. Fission gas swelling and release

Under neutron irradiation, fission gas atoms migrate toward grain boundaries, where they nucleate and growth into nano-scale bubbles inside grains and micron-scale bubbles between grains. When the fission density surpasses a critical threshold, grain recrystallization is triggered[44,47–50], transforming coarse grains into much finer ones. The smaller grain size accelerates the diffusion of fission gases into inter-granular bubbles, thereby promoting further bubble growth. The continuous growth of these bubbles at the grain boundaries gives rise to macroscopic fuel swelling, commonly referred to as fission gas swelling. This irradiation-induced porosity significantly diminishes the macroscale thermo-mechanical performances of nuclear fuels [13,51].

Accurately modeling multi-scale fission gas swelling remains a significant challenge. Based on experimental data, Kim and Hofman [45] expressed fission gas swelling as a function of fission density. Robinson *et al.* [52] conducted similar research; however, these empirical models do not provide a comprehensive understanding of the underlying mechanisms. In pursuit of improved predictive capability, mechanistic frameworks have been established to relate swelling to bubble density and bubble size while incorporating key physical processes [48,53,54]. These physics-based models are capable of accounting for the effects of irradiation temperature, fission rate, and macroscale hydrostatic pressure. However, these models do not account for the deformation of the solid skeleton surrounding the gas bubbles, which cannot reflect the continuum-scale bubble growth mechanism. Jian *et al.* [55], using continuum mechanics, proposed a new model for macroscale volumetric growth strain that incorporates the combined effects of irradiation creep, thermal expansion of the skeleton, and swelling caused by solid fission products. They

also developed a three-dimensional constitutive model and stress update algorithm for multi-scale irradiation-induced deformation and stress analysis. This work reveals the mechanism of fission bubble growth, with its accuracy validated by experimental data (comparison of simulation and experimental results shown in Figure 1 [55]).

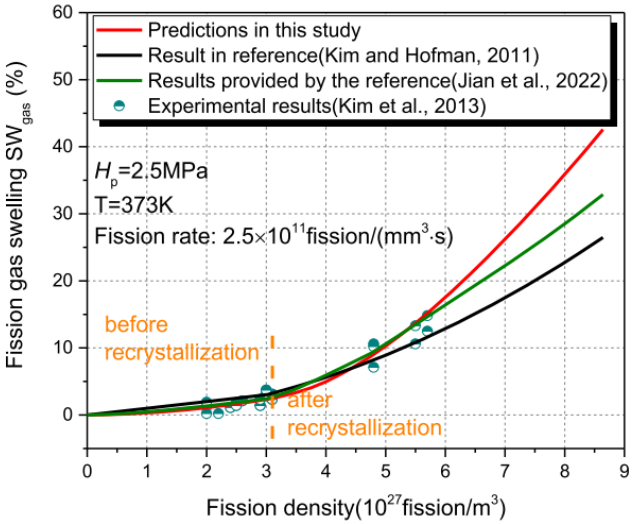

Figure 1. The evolution results of fission gas swelling [55].

In harsh in-pile conditions, gaseous fission products are steadily accumulated in nuclear fuels, ultimately leading to the release of fission gases. The phenomena of fission gas swelling and release are closely interconnected, as both originate from the diffusion-driven migration of fission gas atoms inside the grains of the fuel [56,57]. To capture these coupled effects, Zhang *et al*. [58] developed a model, incorporating the internal pressure of gas bubbles, surface tension effects, external hydrostatic pressure, and creep deformation of the fuel skeleton. This multi-scale framework not only enables accurate predictions of fission gas swelling and release but also reveals that creep-induced damage of the solid skeleton as the primary factor for bubble linkage and gas release. Such mechanistic models, grounded in continuum mechanics and validated against experimental results, provide essential insights for the design and safety assessment of advanced fuel systems.

2.1.3. Thermal conductivity

Thermal conductivity is another critical property of nuclear fuel. Irradiation-induced porous structure significantly reduces the thermal conductivity of nuclear fuel. Burkes *et al.* [51] proposed an empirical model to predict the thermal conductivity of UMo alloys based on factors such as Mo concentration, temperature, and porosity:

$$k_{U-Mo} = 0.25\left[A + \sqrt{A^2 + 8k^0_{U-Mo}k_g}\right] \tag{3}$$

$$A = (1-3P)k^0_{U-Mo} + (3P-1)k_g \tag{4}$$

where, k_{U-Mo} denotes the thermal conductivity (W/m/K) of irradiated U-Mo; k_{U-Mo}^{0} refers to the thermal conductivity (W/m/K) of unirradiated U-Mo. The pores, filled with fission gases such as Xe and Kr, exhibit an effective thermal conductivity k_g (W/m/K). P denotes porosity; and A is a parameter determined by P, k_{U-Mo}^{0} and k_g. Apart from empirical correlations, predictive computational strategies have been utilized to evaluate the thermal conductivity of nuclear materials. Reference [59] discusses the use of the phase-field method to estimate the thermal conductivity of polycrystalline metals containing both inter-granular and intra-granular bubbles. In addition, this investigation examined the impact of microstructural factors—grain size, morphological features, and recrystallization—on macroscale thermal conductivity. This research provides valuable insights for linking the microstructure of nuclear fuel to its macroscale thermo-mechanical properties.

2.1.4. Irradiation-induced creep

Irradiation-induced creep is an important deformation mechanism during the service life of nuclear fuel, leading to damage and accelerating fuel failure. Previous studies on nuclear fuel have primarily focused on UO_2. In recent years, Xie *et al.* [60] analyzed the investigated creep mechanisms in polycrystalline UN and U_3Si_2 fuels. They developed a creep rate model based on vacancy diffusion and dislocation motion mechanisms. The model's predictions closely matched experimental results, validating its accuracy and offering new insights for creep performance research in nuclear fuels [60].

2.1.5. Thermal expansion

During service in the reactor, nuclear fuel experiences temperature rise, leading to thermal expansion and volumetric growth, typically described as

$$SW_{th} = [1 + \alpha(T - T_0)]^3 - 1 \quad (5)$$

where SW_{th} is the volume strain induced by thermal expansion; is the thermal expansion coefficient; T and T_0 are the actual temperature and reference temperature. Numerous researchers have studied the thermal expansion coefficient of nuclear fuel, providing specific values, as shown in References [61,62].

2.1.6. Elastic constants

Elastic constants are important mechanical properties of nuclear fuels, as they are directly related to the mechanical and geometric stability of fuel elements. Numerous researchers [13,63] have experimentally determined the elastic constants of nuclear fuels, including Young's modulus and Poisson's ratio. In service, porosity within nuclear fuels diminishes their effective elastic response. Li *et al.* [9] established the models for the effective elastic constants of irradiated U-10Mo fuel and showed that these constants are primarily governed by the average porosity at the macroscale. Building on this foundation, Jin *et al.* [64] simulated the four-point bending tests of irradiated U-10Mo fuel, formulating models that represent the deterioration of the skeleton Young's modulus as a function of porosity and fission density. The functions are expressed as

$$E_{skeleton} = -6.58903904F_d + 85 \quad (6)$$

$$E_{skeleton} = 4350.12551e^{-\phi/25.4732162} + 16.3690404e^{-\phi/0.0046114} - 4281.4945504 \quad (7)$$

where $E_{skeleton}$ denotes the Young's modulus (GPa) of U-10Mo fuel skeleton; F_d represents the fission density (10^{27} fission/m^3); ϕ indicates the macroscale porosity. Together, these contributions establish a solid basis for accurate modeling of irradiation-induced thermo-mechanical performance in the U-10Mo fuel elements and assemblies.

2.2. Nuclear structural materials

Structural materials exposed to long-time fast neutron irradiation undergo significant degradation in mechanical properties, known as the impact of irradiation damage on mechanical performance [65]. A primary concern is irradiation-induced hardening and embrittlement in structural materials [66]. A combination of numerical simulations, experimental observations, and theoretical modeling plays a key role in understanding irradiation effects [67].

Numerous researchers [68,69] have conducted tensile tests on structural materials, presenting stress-strain curves obtained before and after irradiation, as shown in Figure 2. These studies highlight a post-irradiation reduction in ductility and fracture toughness, along with increases in yield strength and ultimate tensile strength.

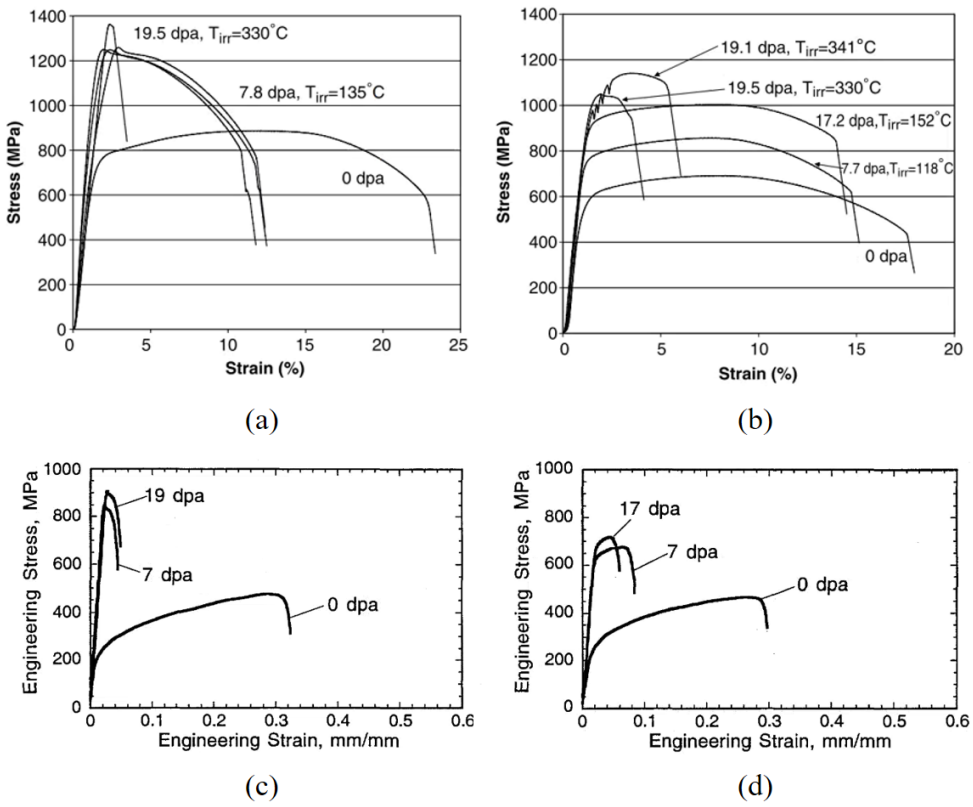

Figure 2. Stress-strain curves measured on **(a)** HT-9 at 25 ℃ [68], **(b)** HT-9 at 250 ℃ [68], **(c)** 316 steel at 330 ℃ [69] and **(d)** 316 steel at 400 ℃ [69].

To investigate irradiation hardening and embrittlement behaviors, crystal plasticity theory and elasto-plastic fracture mechanics are commonly employed [65,70], with model parameters identified using experimental data. It is important to note that the model parameters obtained using these methods do

not necessarily represent the true properties of material points. Ding *et al.* [12] developed a stress-update algorithm based on continuum damage mechanics theory and implemented it through a UMAT subroutine for finite element simulations of circumferential tensile tests, studying hydrogen-induced mechanical degradation behavior in Zr alloys. This research integrated theoretical, numerical, and experimental methods, yielding more reliable mechanical properties for the material points of structural materials.

3. Applications of ML in the development of nuclear materials

The powerful image processing capabilities of ML have been applied to investigate the microstructures of nuclear materials, while its multivariable regression and classification strengths are being applied to model the relationships between processing parameters and macroscale properties. This chapter outlines the application of ML in both the manufacturing processes and microstructural characterization of nuclear materials.

3.1. Nuclear fuel

The macroscale thermo-mechanical properties of nuclear fuels are closely linked to their microstructures, which are strongly influenced by fabrication techniques. Kautz *et al.* [71,72] developed a ML framework to establish quantitative links between processing conditions and microstructural evolution in U-10Mo alloys. Their approach leveraged the powerful feature extraction capabilities of convolutional neural networks (CNNs) [73], employing a pre-trained VGG-19 architecture [74] that was fine-tuned by modifying its fifth convolutional block while freezing the earlier layers [71]. This transfer learning strategy enabled the extraction of high-level image descriptors from a relatively small dataset of 538 microstructure images, yielding compact feature vectors for downstream prediction tasks [71]. The extracted features were subsequently used to predict five annealing conditions (ranging from 500 °C for 0–100 hours) [71] , illustrating how CNNs can serve as a surrogate model for process-structure linkage. Additionally, they applied unsupervised K-means clustering [75] to classify the key microstructural constituents along with their volumetric fractions, with specific image segmentation results shown in Figure 3 [71]. Kautz *et al.* [71,72] highlights the advantage of using pre-trained CNNs for nuclear fuel image analysis where datasets are scarce and expensive to generate. The use of transfer learning effectively circumvents the need to train a deep network from scratch, thereby reducing computational cost and mitigating the risk of overfitting. However, the predictive capacity is constrained by the limited variability of the input parameters. The narrow range of annealing temperatures and durations considered may restrict the generalizability of the model, especially under more complex, multi-step processing conditions. Furthermore, the authors did not explore the interpretability of the CNN features, which remains a crucial barrier in deploying ML models for decision-making in nuclear materials design. In future work, integrating physically informed constraints, such as known phase transformation kinetics, may help enhance the physical reliability of the predictions.

Kautz *et al.* [76] developed a deep neural network (DNN) [77] to predict the thermal conductivity of UMo alloys. The model incorporated 12 input features, including Mo and U enrichment levels, fission density, and temperature, and was structured with eight hidden layers. Seven experimental datasets (AFIP-2BZ-A, AFIP-2BZ-B, AFIP-2BZ-C, AFIP-3BZ-E, AFIP-6II1-H, AFIP-6II1-I, and AFIP-6B-F)

from References [78–80] were used for model training and validation. The trained model indicated that thermal conductivity is most sensitive to Mo enrichment in UMo alloys. The model achieved accurate predictions for AFIP-2BZ-A, AFIP-2BZ-B, AFIP-2BZ-C, and AFIP-6B-F, but exhibited weaker predictive performance for AFIP-3BZ-E, AFIP-6II1-H, and AFIP-6II1-I experiments largely due to insufficient or unbalanced training data, as shown in Figure 4 [76]. This discrepancy underscores the limitations of data-driven models in nuclear materials applications, where the diversity and volume of high-quality experimental data are often restricted by cost, complexity, and safety constraints. The observed degradation in performance is not merely a result of limited data volume, but also of insufficient representativeness in the feature space. In particular, the absence of porosity as an input feature—despite its well-established impact on thermal conductivity [81]—highlights a critical gap in feature engineering. Incorporating microstructural descriptors such as porosity and phase distribution could significantly enhance model fidelity. Moreover, the current DNN architecture lacks embedded physical constraints, which limits its interpretability and extrapolation capability beyond the training domain. As a promising alternative, Physics-Informed Neural Networks (PINNs) [82] offer a way to embed governing equations into the training process, thereby ensuring physically consistent predictions even in low-data regimes. Future work may benefit from hybrid frameworks that couple data-driven inference with physical modeling, leveraging both sparse empirical data and known thermo-physical relationships.

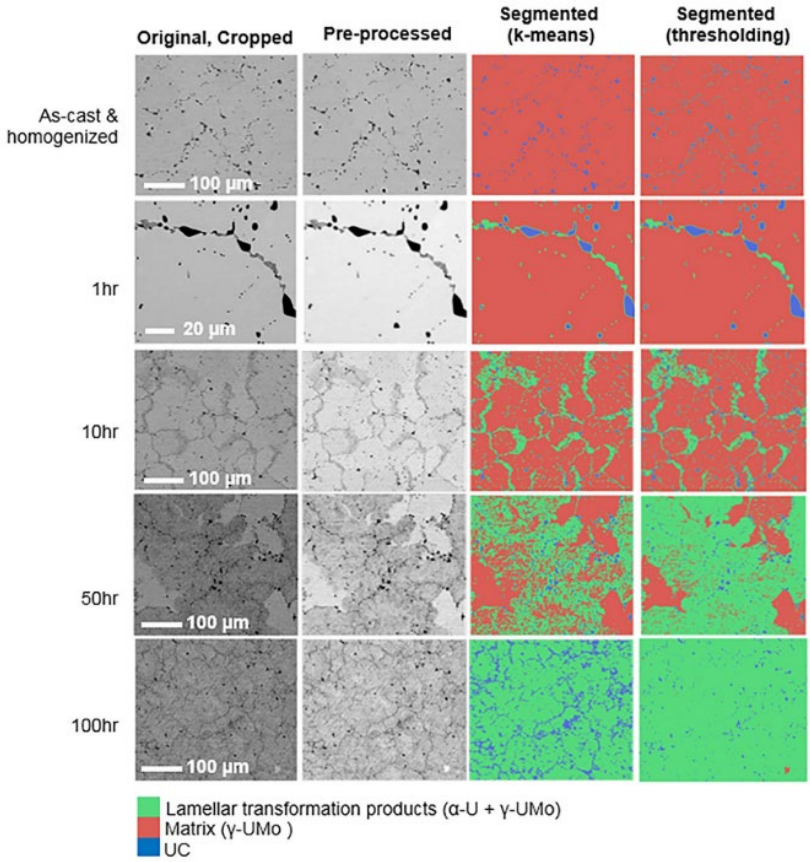

Figure 3. Sample outcomes from k-means [71].

Wei *et al.* [38] proposed a CNN-based approach to extract microstructural feature vectors from porous materials for thermal conductivity prediction. Their model demonstrated reliable accuracy and emphasized the importance of integrating microstructure-sensitive representations into ML workflows.

This suggests that thermal conductivity prediction models for UMo fuels should be multi-modal, combining structured tabular data (e.g., enrichment, temperature) with unstructured image-based features (e.g., porosity maps, grain networks). Such integration could yield more robust and transferable ML models capable of capturing the complex interactions between microstructure and thermal properties in fuels.

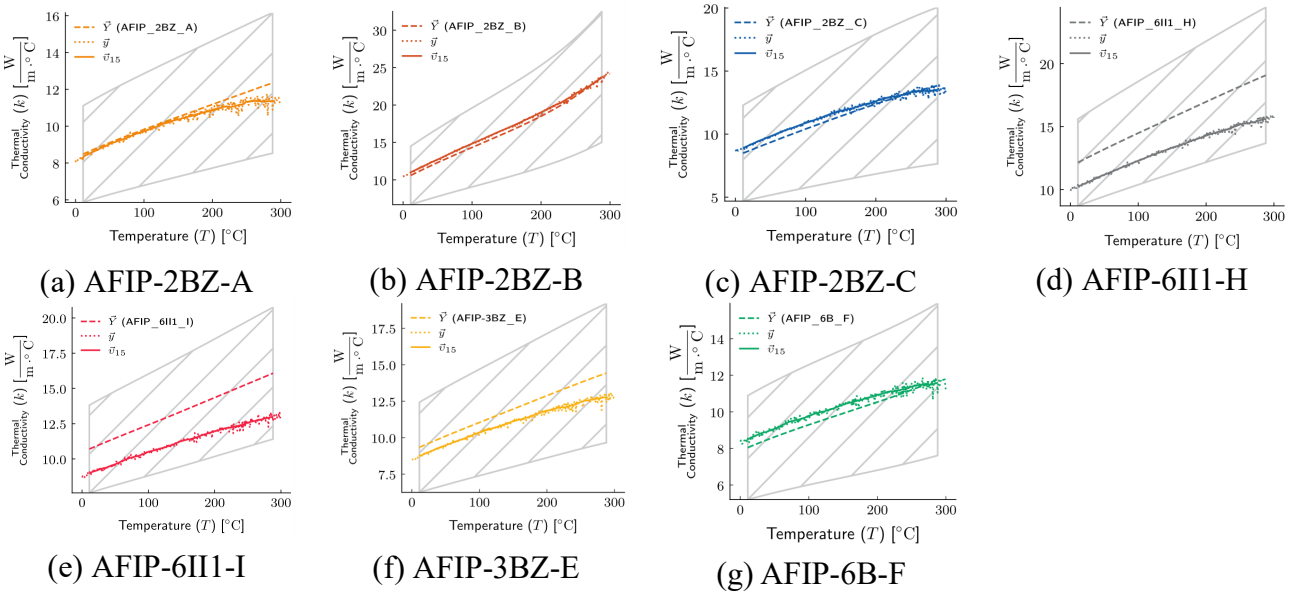

Figure 4. Estimated thermal conductivity of fuel plates. $\vec{Y}$ denotes experimental measurements, $\vec{y}$ corresponds to neural network predictions, and the gray band indicates the uncertainty margin of the computational model [76].

During irradiation, the grain size of UO_2 progressively increases, significantly influencing its thermal conductivity. Therefore, it is essential to study the trend of UO_2 grain size evolution under irradiation and varying temperatures. Yu *et al.* [39] combined manual techniques with ML-based image analysis to quantify grain size variations under irradiation at different temperatures. They employed the U-Net architecture [83], a well-established CNN originally designed for biomedical image segmentation. Its encoder-decoder structure enables precise pixel-wise segmentation, making it particularly suitable for identifying grain boundaries in noisy or low-contrast micrographs typical of irradiated materials. The use of U-Net significantly improved analysis throughput while reducing the labor-intensive nature of manual grain boundary delineation, thereby providing a scalable and reproducible method for microstructural quantification.

In another study, Abbott *et al.* [84] trained an ML model based on the VGG-16 architecture [85] to study the microstructural differences of Am-UO_3, α-UO_3, and U_3O_8 as intermediate products forming UO_2. Despite the fact that these intermediate products yield nearly indistinguishable signals in conventional characterization techniques such as X-ray diffraction (XRD) or X-ray photoelectron spectroscopy (XPS) [84], the ML model achieved a classification accuracy of 97.9 ± 2.1% across the three categories. This finding underscores the unique capability of deep learning methods to extract subtle morphological features that are not readily discernible through traditional analytical methods.

During reactor operation, UO_2 accumulates fission gases, and their release at elevated burnup levels can lead to increased internal rod pressure, posing a threat to cladding integrity and fuel rod failure.

Various factors influence the release of fission gases. Koo *et al.* [86] developed an artificial neural network (ANN) model [87] to forecast fission gas release from UO_2 fuel in light water reactor under reactivity-initiated accident scenarios. The ANN includes five input features and one output (fission gas release amount). A subsequent sensitivity analysis revealed that average fission density is the dominant factor influencing gas release [86]. The proposed model offers a data-driven tool for guiding reactor operation strategies to limit peak power excursions and manage fuel reliability. The application of ML to model gas transport phenomena under extreme conditions demonstrates the potential of neural networks to approximate complex multiphysics behavior when explicit modeling is challenging. However, these models are still constrained by both the volume and reliability of training data, especially in accident scenarios that are difficult to replicate experimentally.

Notably, despite these promising advances, applications of ML to model mechanical properties of nuclear fuels remain underexplored. Although Zhang *et al.* [37] investigated the rapid design of isothermal decomposition parameters for UMo alloys using ML methods, their support vector machine (SVM) model [88] only addressed correlations between processing parameters and alloy hardness based on limited data. More comprehensive mechanical behaviors—such as irradiation-induced creep, swelling, and pellet-cladding interaction—are yet to be systematically investigated using ML approaches. The primary challenges lie in the complex irradiation-induced thermo-mechanical behaviors, the scarcity of high-fidelity mechanical property data under irradiation, and the need to embed physical equations into data-driven models. Moreover, the in-reactor behaviors of nuclear fuels are influenced by a wide array of interacting factors—such as temperature gradients, fission gas behavior, microstructural evolution, fission rate, and irradiation damage accumulation—making it extremely difficult to determine which features should be included as reliable and physically meaningful inputs. Improper input selection or omission of critical variables can lead to inaccurate predictions and severely limit model generalization. Thus, the identification and engineering of representative features that faithfully capture the underlying physics is itself a major challenge for ML applications in this field.

3.2. Nuclear structural materials

The metal-water chemical reaction during reactor operation results in hydrogen pickup in zirconium alloy cladding tubes, compromising their failure resistance [12]. Improving the strength and ductility of cladding materials and extending their service life is essential for the safe operation of reactors. Zirconium oxide film porosity governs corrosion dynamics and oxidation of Zr alloys, with increased porosity adversely affecting the fracture behavior of Zr alloys. Zhang *et al.* [41] developed a CNN to extract the micro-porosity of the oxide film on Zr alloys. CNN architectures are highly effective for this task because they can detect hierarchical patterns and spatial features in complex image datasets. The porosity values predicted by the model closely matched those obtained from manual image analysis, both in terms of trend and magnitude, while drastically improving processing speed and consistency. The chemical composition of Zr alloys also substantially impacts their macroscale mechanical properties. Si *et al.* [40] investigated the mechanical behavior of Zr-Ti-Nb-O alloys using a random forest regression model, which is particularly effective for handling non-linear data with complex feature interactions. By incorporating variables such as crystal structure parameters, solid solution strengthening effects, and dislocation mobility indicators, their model provided valuable insights into the compositional and microstructural factors influencing yield strength and plasticity. Despite these achievements, current

studies remain limited in several respects. The corrosion and mechanical degradation of Zr alloys are time-dependent, environment-sensitive processes involving complex interactions among chemical, thermal, and mechanical fields. Most existing ML models rely on static datasets and lack the ability to capture temporal evolution or environmental feedback mechanisms. Future work should focus on integrating time-series data to more comprehensively model the degradation behavior of Zr alloys.

SiC/SiC composites are a novel high-strength, high-temperature-resistant ceramic material characterized by low density, excellent thermal stability, corrosion resistance, and outstanding mechanical properties, making them a promising candidate for cladding applications. However, processing ceramic-based materials poses significant challenges. Some researchers have proposed using water-jet guided nanosecond lasers [89] to facilitate SiC/SiC machining, which offers improved precision and reduced thermal damage. Gao *et al.* [90] developed a DNN to investigate how laser processing parameters influence results, thus enabling more efficient optimization of SiC/SiC fabrication. Interestingly, in this study [90] it was found that under low pulse energy (0–10 W), increasing the laser scanning speed improved processing quality—contrary to conventional physical models, which predict lower quality due to reduced heat input. This highlights the unique advantage of ML: its ability to capture latent patterns in high-dimensional experimental data that may elude conventional analytical frameworks. Because SiC/SiC is a brittle material, any damage can lead to rapid structural failure of the cladding due to stress concentration effects from cracks. Zhang *et al.* [91] utilized the U-Net architecture for image segmentation to study damage modes such as matrix cracking, delamination, fiber fracture, and fiber pull-out in SiC/SiC under various load conditions, with examples of segmentation results shown in Figure 5. U-Net's encoder-decoder architecture is particularly suited for this task, as it enables pixel-wise localization of complex morphological features within composite micrographs. The segmentation results enable quantitative damage assessment and offer a foundation for subsequent failure modeling.

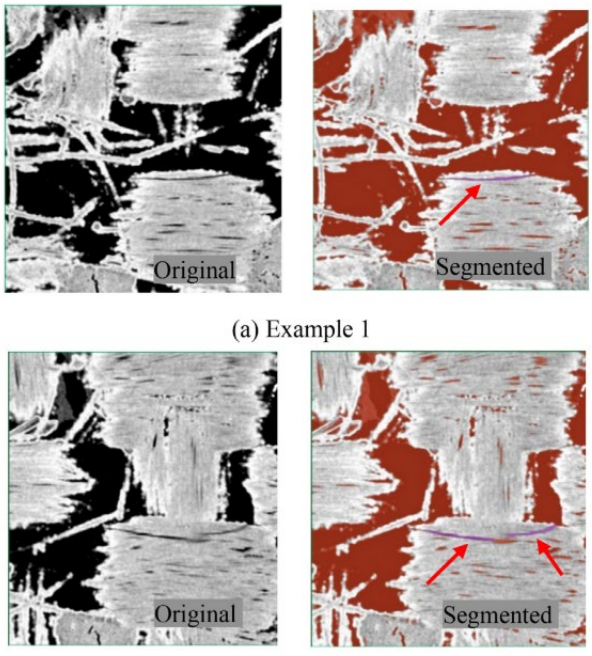

Figure 5. Examples of segmentation results using U-Net [91].

In a complementary effort, Patel *et al.* [92] developed a neural network to predict the probability of transverse crack initiation in SiC/SiC composites based on microstructural morphology. To overcome the scarcity of experimental crack data, they generated synthetic training datasets using high-fidelity finite element simulations, thereby establishing a surrogate ML model that can estimate damage likelihood as a function of local microstructure. This approach demonstrates the potential of integrating physics-based simulations with ML to create predictive models that are both data-efficient and physically grounded. Furthermore, ML has also been applied to the non-destructive evaluation of SiC/SiC composites. Several studies [42,43,93] have applied ML in conjunction with ultrasonic testing data to detect internal damage and estimate residual strength. These data-driven diagnostic tools provide valuable support for real-time health monitoring, in-service assessment, and integrity management of structural components in nuclear environments.

Chao *et al.* [94] proposed a backpropagation neural network (BPNN) [95] to fit creep curves, oxidation gain (or loss) curves, and residual strength under different stress, temperature, and environmental conditions for SiC/SiC composites. Their numerical experiments on univariate and multivariate data demonstrated the improved predictive performance of this model. However, it is important to note that the BPNN trained by Chao *et al.* [94] used a small dataset and potentially biased toward specific test conditions. As a result, the generalization capability of the model to unseen operational regimes remains unproven.

3.3. Integrating FEM and ML for nuclear material properties prediction

Due to the high cost, limited scalability, and inherent safety challenges of irradiation experiments for nuclear materials, finite element methods (FEM), based on validated physics-based constitutive models, have become an indispensable tool for simulating microstructural evolution and material behavior under various conditions. FEM not only serves as a powerful stand-alone tool, but also provides high-fidelity synthetic datasets to train data-driven ML models. When effectively trained, ML models can function as computationally efficient surrogate models, offering rapid predictions of material response while retaining fidelity to the underlying physical phenomena. Fu *et al.* [96] demonstrated this integration by modeling the hot rolling and annealing process of UMo fuel alloys. They selected seven key processing parameters input features such as total reduction, heat treatment time, and the number of hot rolling passes. A DNN was then trained to predict four outcomes, including final grain size and recrystallization percentage, based on these processing features. This work extends earlier image-based microstructural modeling studies by Kautz *et al.* [71,72], but shifts the focus toward process-structure relationships via physics-informed simulations. Notably, Fu *et al.* [96] used FEM simulations of the manufacturing process to create a dataset, replacing experimental results with numerical simulation data. This approach, summarized in Figure 6. The successful implementation of this framework primarily relies on an existing physics-based model [97,98] developed to describe the rolling process. Accurate physical models are essential to ensure that FEM simulations produce results reliable enough to substitute for experiments, thus enabling the development of trustworthy ML surrogate models. Compared to the conventional physics-based simulations, the ML surrogate model developed by Fu *et al.* [96] offers a remarkable speed-up—by a factor of 1000—demonstrating strong potential for optimizing the fabrication process of U-10Mo. This study confirms the feasibility of integrating FEM with ML for investigating nuclear material behavior, significantly reducing experimental costs and greatly improving analysis efficiency.

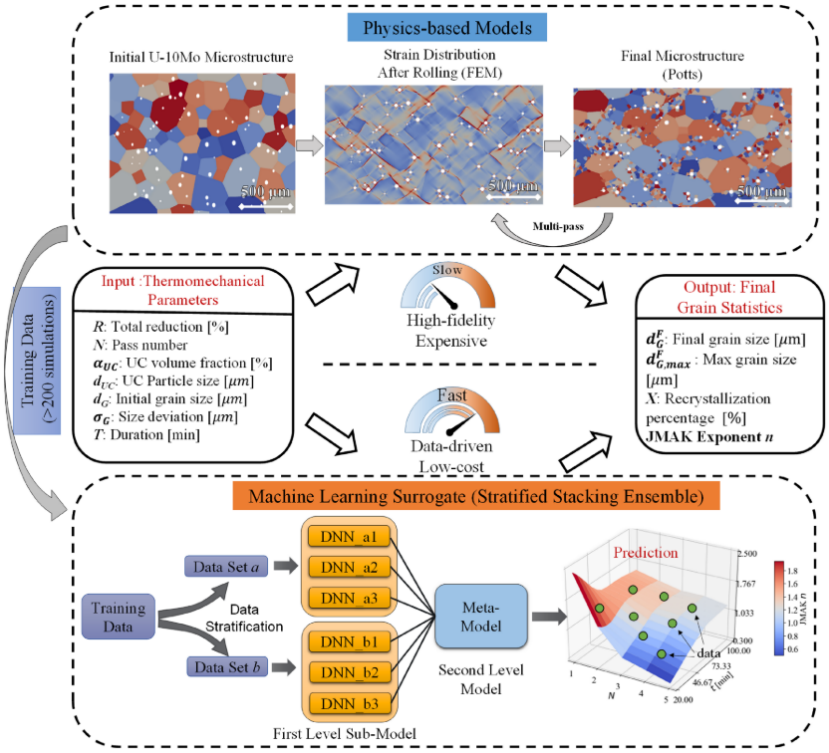

Figure 6. Strategy combining physics simulations and data-driven surrogates for sensitivity analysis and efficient prediction and optimization of U-10Mo microstructure [96].

Building upon the integration of FEM-generated datasets and ML models, Yan *et al.* [99] conducted an optimization study on the thermal conductivity of UO_2-Mo composites. They constructed a dataset based on FEM simulation results, incorporating 12 input features such as Mo volume fraction (MF), crack volume fraction (CF), and others [99]. Multiple ML algorithms were evaluated for their regression performance, including ANN, SVM, gaussian process regression (GPR), and gradient-boosted decision trees (GBDTs) [100]. Among them, the ANN and GBDT models exhibited the highest predictive accuracy [99], as shown in Figure 7. An additional benefit of the tree-based models lies in their inherent ability to assess input feature importance. Feature attribution analysis (Figure 8) [99] indicated that the MF is the most critical factor affecting the effective thermal conductivity of the UO_2–Mo composite, which is consistent with physical expectations given the high intrinsic conductivity of Mo compared to UO_2 [99]. This study underscores the advantage of ML models in not only making accurate predictions but also offering interpretable insights into structure–property relationships. In their subsequent work, Yan *et al.* [101] proposed a bidirectional predictive DNN, linking the structural characteristics of composite fuels to their effective thermal conductivity. This model could predict the thermal conductivity of UO_2 based on given structural features and inversely infer structural features from a target thermal conductivity, thereby accelerating the fuel design process and reducing development costs. Such inverse design frameworks, when trained on high-fidelity FEM data, hold immense potential for navigating the complex design space of composite fuels. Further advancing this predictive paradigm, Gong *et al.* [39] employed a well-established CNN model (ResNet101) [102], leveraging its powerful capability to extract microstructural features of UO_2-BeO and establish correlations with thermal conductivity, further refining the predictive framework for UO_2 thermal conductivity. Overall, these studies offer innovative and practical approaches to the

development of advanced composite fuels, significantly accelerating their design and reducing associated costs.

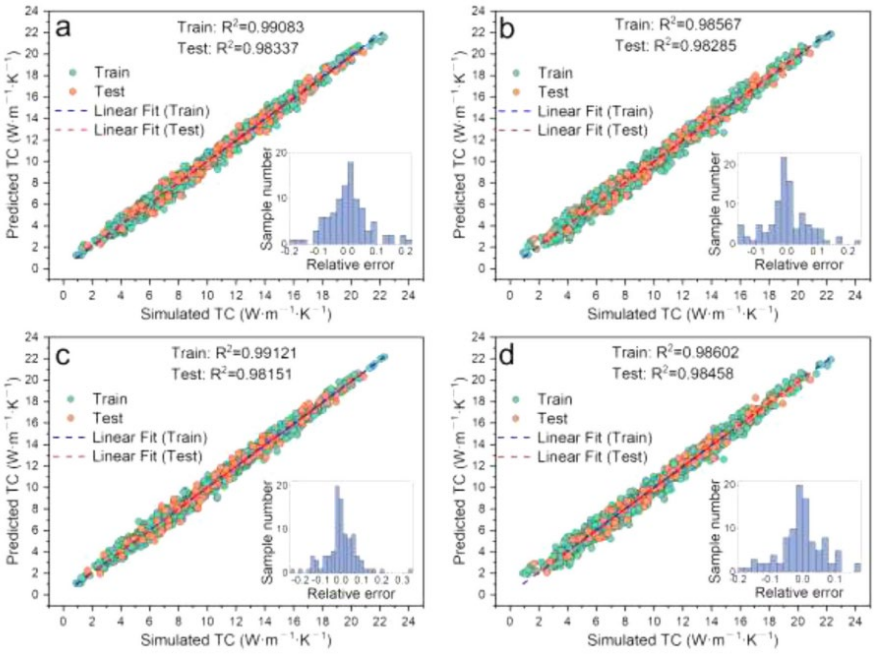

Figure 7. Regression plots comparing FEM-simulated thermal conductivity with thermal conductivity predicted by various ML models. **(a)** GBDTs; **(b)** SVM; **(c)** GPR; **(d)** ANN [99].

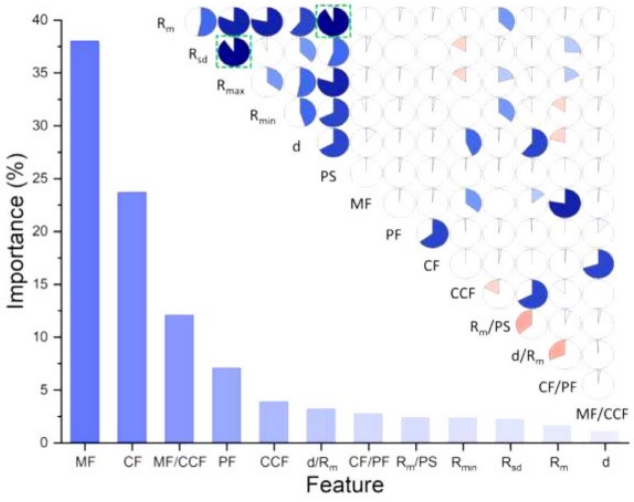

Figure 8. The importance of different features on thermal conductivity, and the meanings of the abbreviations for the features in the figure can be found in Reference [99].

Recent advances in high-throughput modeling and data-driven approaches have enabled more efficient exploration of structure–property relationships in complex nuclear fuel systems. Dong *et al.* [103] investigated the impact of particle agglomeration on the equivalent mechanical properties of dispersion nuclear fuel using a combination of numerical simulations and ML. They developed an automated computational workflow that integrates parametric modeling, parallelized finite element simulations, and post-processing to generate a large-scale dataset characterizing the mechanical behavior of dispersion fuel microstructures with varying particle distributions. By employing a Fourier distribution

function to describe the spatial configuration of randomly dispersed fuel particles, the study systematically analyzed how key microstructural features—such as particle distribution, volume fraction, and degree of agglomeration—affect the maximum von Mises stress of the fuel skeleton and effective Young's modulus. The resulting high-throughput dataset was then used to train a GPR model, which successfully predicted the mechanical properties of unseen configurations with high accuracy. In particular, the ability to capture the influence of particle agglomeration—an effect that is difficult to parameterize in conventional analytical models—highlights the strength of ML in modeling stochastic microstructural phenomena. This work demonstrates the potential of integrating ML with automated simulation pipelines to efficiently characterize the mechanical performance of complex composite fuel structures.

Similar approaches have also been applied to the investigation of nuclear structural material properties. Zikry *et al*. [104,105]developed the dislocation-density crystalline approach. Building on this framework, Hasan *et al*. [106] generated a dataset through finite element simulations. They subsequently developed a method using GPR to predict the link between the fracture stress and probability of failure under different strain levels, as shown in Figure 9. GPR was selected for its non-parametric, probabilistic nature, which enables uncertainty quantification and captures complex, nonlinear trends even in sparse datasets. Their findings indicated that fracture probability is primarily governed by hydride orientation and the coupled effect with dislocation density. This work reinforces the feasibility and value of using FEM-based simulation data to train ML models in cases where experimental characterization is either impractical or insufficient.

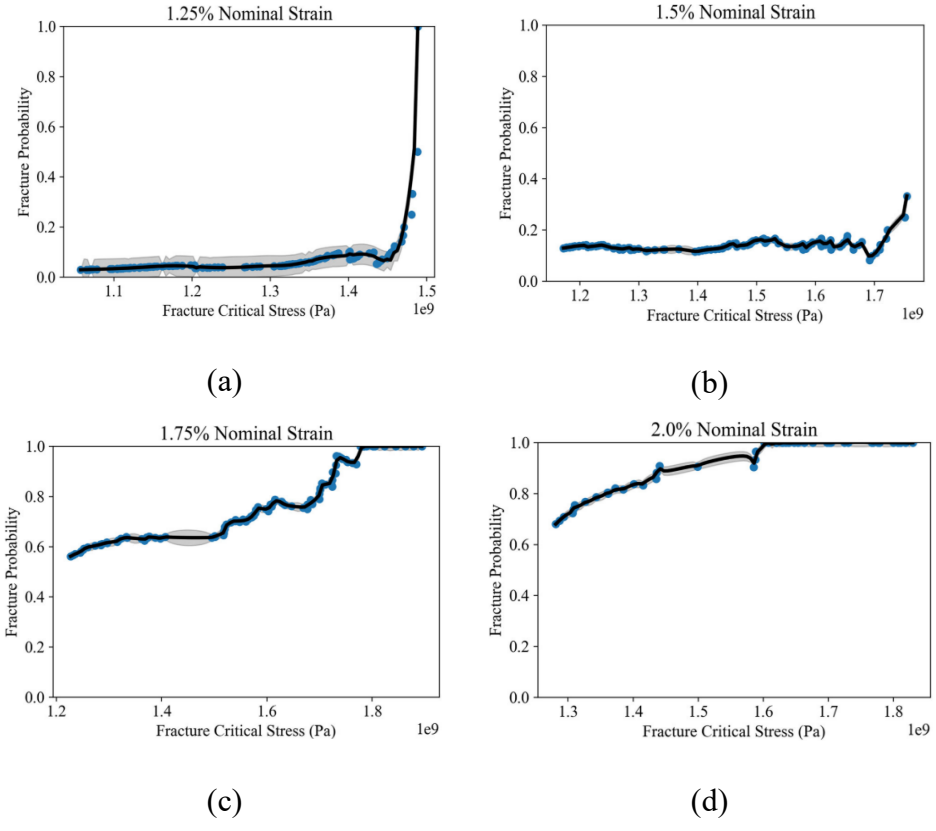

Figure 9. GPR fitting of failure probability for fracture stress at **(a)** 1.25%, **(b)** 1.5%, **(c)** 1.75% and **(d)** 2.0% nominal strain [106].

In summary, the combined use of FEM and ML constitutes a powerful framework for modeling both fuel and structural material behavior. While ML provides computational speed and flexibility, FEM contributes physical rigor and interpretability. This synergy offers a promising direction for addressing the multi-scale, multi-physics challenges associated with nuclear materials design, optimization, and qualification.

4. Conclusion and future outlook

This review explores the extensive applications of ML in the investigation of nuclear material properties. First, powerful image processing techniques such as CNN and K-means algorithms have been widely used to extract microstructural information for nuclear materials. These techniques significantly enhance data analysis efficiency, providing crucial support for the design and optimization of nuclear material processing techniques. Secondly, ML has found broad application in research concerning the thermal conductivity of nuclear materials. ML models can rapidly predict thermal conductivity by learning from existing data, thereby accelerating material design and selection processes.

Additionally, transfer learning models and FEM are also widely used in nuclear material research. These methods effectively address the issue of limited experimental data. ML techniques also exhibit strong potential in investigating the mechanical behavior of nuclear materials, including creep deformation and failure mechanisms. By analyzing large volumes of datasets, ML models can predict the degradation trends of materials over long service periods, thereby guiding material design and optimization. Overall, ML has been proven to be a reliable and efficient tool, contributing significantly to advancements in nuclear material science.

Despite these successes, significant challenges remain. Irradiation-induced thermo-mechanical interactions in nuclear materials is governed by highly complex, multiscale physical phenomena. A key difficulty lies in selecting representative and physically meaningful input features, ensuring that critical variables such as porosity and creep strain are not overlooked. Progress is further constrained by the limited availability of robust, high-quality datasets, impeding the construction of ML models capable of wide applicability. Moving forward, future investigations should prioritize addressing these limitations by focusing on:

(1) Developing hybrid ML-physics frameworks that embed physical constraints, governing equations, and mechanistic insights into the training process;

(2) Incorporating temporal and spatial correlations through recurrent or attention-based architectures for modeling time-dependent behaviors;

(3) Expanding inverse design capabilities, enabling researchers to identify optimal compositions or microstructures based on target properties;

(4) Generating diverse and physics-informed datasets via finite element simulations.

In the future, as ML technology continues to evolve and mature, its application prospects in nuclear material research will become even broader. By integrating ML with cutting-edge computational methodologies, researchers are poised to make substantial breakthroughs in nuclear material design, performance prediction, and in-service behavior analysis, thereby establishing a more robust foundation for the safe, reliable, and efficient utilization of nuclear energy.

Acknowledgments

The authors thank for the supports of National Natural Science Foundation of China (Nos. 12132005, 12135008, 12102094).

Authors' contribution

Chaoyue Jin: conceptualization, methodology, investigation, writing—original draft preparation; Shurong Ding: conceptualization, supervision, project administration, funding acquisition, writing—review and editing. All authors have read and agreed to the published version of the manuscript.

Conflicts of interests

The authors declare no conflict of interest.

References

[1] Chu S, Majumdar A. Opportunities and challenges for a sustainable energy future. *Nature* 2012, 488(7411):294–303.

[2] Deutch JM, Forsberg CW, Kadak AC, Kazimi MS, *et al.* Update of the MIT 2003 future of nuclear power. 2009. Available: http://large.stanford.edu/courses/2017/ph241/kim-d2/docs/nuclearpower-update2009.pdf (accessed on 13 August 2025).

[3] Li H, Sun X, Li L. The enlightenment brought by the European energy crisis to China's nuclear energy development (in Chinese). *Energy China* 2022,9:57–68.

[4] Wang G, Wang Z, Yun D. Cladding failure modelling for lead-based fast reactors: a review and prospects. *Metals* 2023, 13(9):1524.

[5] Morgan D, Pilania G, Couet A, Uberuaga BP, Sun C*, et al.* Machine learning in nuclear materials research. *Curr. Opin. Solid State Mater. Sci.* 2022, 26(2):100975.

[6] Friedman SM. Three Mile Island, Chernobyl, and Fukushima: an analysis of traditional and new media coverage of nuclear accidents and radiation. *Bull. At. Sci.* 2011, 67(5):55–65.

[7] Sorbom BN, Ball J, Palmer TR, Mangiarotti FJ, Sierchio JM*, et al.* ARC: a compact, high-field, fusion nuclear science facility and demonstration power plant with demountable magnets. *Fusion Eng. Des.* 2015, 100:378–405.

[8] Kuang AQ, Cao NM, Creely AJ, Dennett CA, Hecla J, *et al.* Conceptual design study for heat exhaust management in the ARC fusion pilot plant. *Fusion Eng. Des.* 2018, 137:221–242.

[9] Li Y, Ding G, Xie Z, Zhang J, Jian X, *et al.* Models for effective elastic constants of irradiated U-10Mo fuels with distributed fission gas bubbles. *J. Nucl. Mater.* 2023, 579:154359.

[10] Zhong Y, Gao R, Li B, Yang Z, Huang Q, *et al.* Preparation and characterization of large grain UO2 for accident tolerant fuel. *Front. Mater.* 2021, 8:651074.

[11] Xia Z, Zhang J, Tong Q, Ding S. Multi-physics modeling of delayed hydride cracking in zirconium alloys, *J. Mech. Phys. Solids* 2019, 132:103677.

[12] Ding G, Zhang J, Wang J, Li Y, Jian X, *et al.* Modeling and tests on the damage and fracture behaviors of non-irradiated zirconium alloys with different hydrogen concentrations at RT and 350 °C. *J. Nucl. Mater.* 2023, 587:154726.

[13] Schulthess JL, Lloyd WR, Rabin B, Wheeler K, Walters TW. Mechanical properties of irradiated UMo alloy fuel. *J. Nucl. Mater.* 2019, 515:91–106.
[14] Schulthess J, Heighes M, Michelich C, Adkins C, Marshall MC, *et al.* Mechanical and thermophysical properties of low enriched uranium-10wt% molybdenum rolled foils. *J. Nucl. Mater.* 2022, 563:153628.
[15] Schulthess J, Lloyd R, Rabin B, Heighes M, Trowbridge T, *et al.* Elevated temperature tensile tests on DU–10Mo rolled foils. *J. Nucl. Mater.* 2018, 510:282–296.
[16] Ren C, Yang Y, Li Y, Huai P, Zhu Z, *et al.* Sample spinning to mitigate polarization artifact and interstitial-vacancy imbalance in ion-beam irradiation. *npj Comput. Mater.* 2020, 6(1):189.
[17] Zarei M. On a reduced order modeling of the nuclear reactor dynamics. *Appl. Math. Comput.* 2021, 393:125819.
[18] Khan MJH, Alam A, Ahsan MH, Mamun KAA, Islam SMA. Validation study of the reactor physics lattice transport code WIMSD-5B by TRX and BAPL critical experiments of light water reactors. *Ann. Nucl. Energy* 2015, 85:1014–1017.
[19] Gao S, Leslie DC, Hewitt GF. Improvements to the modelling of two-phase flow and heat transfer in a transient nuclear reactor analysis code. *Appl. Therm. Eng.* 2008, 28(8–9):915–922.
[20] Derenzo SE, Boswell MS, Bourret-Courchesne E, Boutchko R, Budinger TF, *et al.* Design and implementation of a facility for discovering new scintillator materials. *IEEE Trans. Nucl. Sci.* 2008, 55(3):1458–1463.
[21] Stein HS, Gregoire JM. Progress and prospects for accelerating materials science with automated and autonomous workflows. *Chem. Sci.* 2019, 10(42):9640–9649.
[22] Sanderson K. Automation: chemistry shoots for the Moon. *Nature* 2019, 568(7753):577–579.
[23] LeCun Y, Bengio Y, Hinton G. Deep learning. *Nature* 2015, 521(7553):436–444.
[24] Hkdh B. Neural networks in materials science. *ISIJ Int.* 1999, 39(10):966–979.
[25] Ashby MF. Materials selection in mechanical design. *Metall. Ital.* 1994, 86:475–475.
[26] Shi Z, Tsymbalov E, Dao M, Suresh S, Shapeev A, *et al.* Deep elastic strain engineering of bandgap through machine learning. *Proc. Natl. Acad. Sci. U.S.A.* 2019, 116(10):4117–4122.
[27] Tsymbalov E, Shi Z, Dao M, Suresh S, Li J, *et al.* Machine learning for deep elastic strain engineering of semiconductor electronic band structure and effective mass. *npj Comput. Mater.* 2021, 7(1):76.
[28] Li J. EML webinar overview: elastic strain engineering for unprecedented properties. *Extreme Mech. Lett.* 2022, 54:101430.
[29] Kim E, Huang K, Saunders A, McCallum A, Ceder G, *et al.* Materials synthesis insights from scientific literature via text extraction and machine learning. *Chem. Mater.* 2017, 29(21):9436–9444.
[30] Forrester A, Sobester A, Keane A. *Engineering design via surrogate modelling: a practical guide*, 1st ed. Hoboken: John Wiley & Sons, 2008.
[31] Razavi S, Tolson BA, Burn DH. Review of surrogate modeling in water resources. *Water Resour. Res.* 2012, 48(7).
[32] Queipo NV, Haftka RT, Shyy W, Goel T, Vaidyanathan R, *et al.* Surrogate-based analysis and optimization. *Prog. Aerosp. Sci.* 2005, 41(1):1–28.
[33] Pan S, Yang Q. A survey on transfer learning. *IEEE Trans. Knowl. Data Eng.* 2009, 22(10):1345–1359.
[34] Weiss K, Khoshgoftaar TM, Wang D. A survey of transfer learning. *J. Big Data* 2016, 3(1):9.

[35] Zhuang F, Qi Z, Duan K, Xi D, Zhu Y, *et al.* A comprehensive survey on transfer learning. *Proc. IEEE* 2020, 109(1):43–76.

[36] Tan C, Sun F, Kong T, Zhang W, Yang C, *et al.* A survey on deep transfer learning. *In International conference on artificial neural networks*, 1st ed. Cham: Springer International Publishing, 2018. pp. 270–279.

[37] Zhang X, Kang S, Wang Z, Dong Q, Liu W, *et al.* Machine learning assisted design of isothermal decomposition parameters of U-Mo alloy. *Rare Met. Mater. Eng.* 2020, 49(11):3835–3840.

[38] Wei H, Zhao S, Rong Q, Bao H. Predicting the effective thermal conductivities of composite materials and porous media by machine learning methods. *Int. J. Heat Mass Transfer* 2018, 127:908–916.

[39] Yu Z, Xu X, Chen W, Sharma Y, Wang X, *et al. In-situ* irradiation-induced studies of grain growth kinetics of nanocrystalline UO2. *Acta Mater.* 2022, 231:117856.

[40] Si S, Fan B, Liu X, Zhou T, He C, *et al.* Study on strengthening effects of Zr-Ti-Nb-O alloys via high throughput powder metallurgy and data-driven machine learning. *Mater. Des.* 2021, 206:109777.

[41] Zhang H, Kim T, Swarts J, Yu Z, Su R, *et al.* Nano-porosity effects on corrosion rate of Zr alloys using nanoscale microscopy coupled to machine learning. *Corros. Sci.* 2022, 208:110660.

[42] Louis SYM, Nasiri A, Bao J, Cui Y, Zhao Y, *et al.* Remaining useful strength (RUS) prediction of SiCf-SiCm composite materials using deep learning and acoustic emission. *Appl. Sci.* 2020, 10(8):2680.

[43] Muir C, Swaminathan B, Fields K, Almansour AS, Sevener K, *et al.* A machine learning framework for damage mechanism identification from acoustic emissions in unidirectional SiC/SiC composites. *npj Comput. Mater.* 2021, 7(1):146.

[44] Liang L, Mei ZG, Yacout AM. Fission-induced recrystallization effect on intergranular bubble-driven swelling in U-Mo fuel. *Comput. Mater. Sci.* 2017, 138:16–26.

[45] Kim YS, Hofman GL. Fission product induced swelling of U–Mo alloy fuel. *J. Nucl. Mater.* 2011, 419(1–3):291–301.

[46] Suzuki M, Saitou H. Light water reactor fuel analysis code FEMAXI-V (Ver. 1). 2003. Available: https://inis.iaea.org/records/j8xne-09558 (accessed on 13 August 2025).

[47] Kim YS, Hofman GL, Cheon JS. Recrystallization and fission-gas-bubble swelling of U–Mo fuel. *J. Nucl. Mater.* 2013, 436(1–3):14–22.

[48] Rest J. A model for the influence of microstructure, precipitate pinning and fission gas behavior on irradiation-induced recrystallization of nuclear fuels. *J. Nucl. Mater.* 2004, 326(2–3):175–184.

[49] Rest J. A model for the effect of the progression of irradiation-induced recrystallization from initiation to completion on swelling of UO2 and U–10Mo nuclear fuels. *J. Nucl. Mater.* 2005, 346(2–3):226–232.

[50] Rest J. Evolution of fission-gas-bubble-size distribution in recrystallized U–10Mo nuclear fuel. *J. Nucl. Mater.* 2010, 407(1):55–58.

[51] Burkes DE, Casella AM, Casella AJ, Buck EC, Pool KN, *et al.* Thermal properties of U–Mo alloys irradiated to moderate burnup and power. *J. Nucl. Mater.* 2015, 464:331–341.

[52] Robinson AB, Williams WJ, Hanson WA, Rabin BH, Lybeck NJ, *et al.* Swelling of U-Mo monolithic fuel: developing a predictive swelling correlation under research reactor conditions. *J. Nucl. Mater.* 2021, 544:152703.

[53] Cui Y, Ding S, Chen Z, Huo Y. Modifications and applications of the mechanistic gaseous swelling model for UMo fuel. *J. Nucl. Mater.* 2015, 457:157–164.

[54] Jian X, Yan F, Kong X, Ding S. Further development of the fission gas swelling model for U-10Mo fuels. *J. Nucl. Mater.* 2022, 565:153769.

[55] Jian X, Zhang J, Li Y, Ding S. Skeleton-creep based bubble growth model and multi-scale mechanical constitutive model for U-10Mo fuels under irradiation. *Int. J. Plast.* 2023, 163:103557.

[56] Lösönen P. Modelling intragranular fission gas release in irradiation of sintered LWR UO2 fuel. *J. Nucl. Mater.* 2002, 304(1):29–49.

[57] Khvostov G, Mikityuk K, Zimmermann MA. A model for fission gas release and gaseous swelling of the uranium dioxide fuel coupled with the FALCON code. *Nucl. Eng. Des.* 2011, 241(8):2983–3007.

[58] Zhang J, Yan F, Ding S. Continuum-mechanics-based multi-scale modeling of fission gas swelling and release coupling behaviors for UO2 fuels. *J. Nucl. Mater.* 2025, 609:155757.

[59] Hu S, Casella AM, Lavender CA, Senor DJ, Burkes DE. Assessment of effective thermal conductivity in U–Mo metallic fuels with distributed gas bubbles. *J. Nucl. Mater.* 2015, 462:64–76.

[60] Xie Z, Yin C, Zhang J, Jiao Y, Ding G, *et al.* On the creep mechanisms and macroscopic creep rate modeling of high-uranium-density composite fuels. *J. Nucl. Mater.* 2023, 586:154679.

[61] Robinson AB, Wachs DM, Burkes DE, Keiser DD. US RERTR fuel development post irradiation examination results. 2008. Available: https://inldigitallibrary.inl.gov/sites/sti/sti/4282340.pdf (accessed on 13 August 2025).

[62] Siefken LJ, Coryell EW, Harvego EA, Hohorst JK. MATPRO-a library of materials prop erties for light-water-reactor accident analysis. 2001. Available: https://www.nrc.gov/docs/ML0103/ML010330363.pdf (accessed on 13 August 2025).

[63] Kim YS, Hofman GL, Cheon JS, Robinson AB, Wachs DM. Fission induced swelling and creep of U–Mo alloy fuel. *J. Nucl. Mater.* 2013, 437(1–3):37–46.

[64] Jin C, Xie Z, Chen L, Chen X, Zhang J, *et al*. On the degradation of young's modulus of irradiated U-10Mo. *J. Nucl. Mater.* 2025, 610:155799.

[65] Xiao X, Terentyev D, Chu H, Duan H. Theoretical models for irradiation hardening and embrittlement in nuclear structural materials: a review and perspective. *Acta Mech. Sin.* 2020, 36:397–411.

[66] Li M, Eldrup M, Byun TS, Hashimoto N, Snead LL, *et al.* Low temperature neutron irradiation effects on microstructure and tensile properties of molybdenum. *J. Nucl. Mater.* 2008, 376(1):11–28.

[67] Knaster J, Moeslang A, Muroga T. Materials research for fusion. *Nat. Phys.* 2016, 12(5):424–434.

[68] Maloy SA, Romero T, James MR, Dai Y. Tensile testing of EP-823 and HT-9 after irradiation in STIP II. *J. Nucl. Mater.* 2006, 356(1–3):56–61.

[69] Robertson JP, Rowcliffe AF, Grossbeck ML, Ikuo I, Shiro J. Temperature dependence of the deformation behavior of type 316 stainless steel after low temperature neutron irradiation. 1996. Available: https://inis.iaea.org/records/1qzer-40a55 (accessed on 13 August 2025).

[70] Scibetta M, Ferreno D, Gorrochategui I, Lacalle R, Van Walle E, *et al.* Characterisation of the fracture properties in the ductile to brittle transition region of the weld material of a reactor pressure vessel. *J. Nucl. Mater.* 2011, 411(1–3):25–40.

[71] Kautz E, Ma W, Jana S, Devaraj A, Joshi V, *et al.* An image-driven machine learning approach to kinetic modeling of a discontinuous precipitation reaction. *Mater. Charact.* 2020, 166:110379.

[72] Ma W, Kautz EJ, Baskaran A, Chowdhury A, Joshi V, *et al.* Image-driven discriminative and generative machine learning algorithms for establishing microstructure–processing relationships. *J. Appl. Phys.* 2020, 128(13):134901.

[73] O'shea K, Nash R. An introduction to convolutional neural networks. *arXiv* 2015, arXiv:1511.08458.

[74] Tajbakhsh N, Shin JY, Gurudu SR, Hurst RT, Kendall CB, *et al.* Convolutional neural networks for medical image analysis: full training or fine tuning? *IEEE Trans. Med. Imaging* 2016, 35(5):1299–1312.

[75] Krishna K, Murty MN. Genetic K-means algorithm. *IEEE Trans. Syst., Man, Cybern. B, Cybern.* 1999, 29(3):433–439.

[76] Kautz EJ, Hagen AR, Johns JM, Burkes DE. A machine learning approach to thermal conductivity modeling: a case study on irradiated uranium-molybdenum nuclear fuels. *Comput. Mater. Sci.* 2019, 161:107–118.

[77] Samek W, Binder A, Montavon G, Lapuschkin S, Müller KR. Evaluating the visualization of what a deep neural network has learned. *IEEE Trans. Neural Networks Learn. Syst.* 2016, 28(11):2660–2673.

[78] Perez DM, Lillo MA, Chang GS, Wools NE. RERTR-12 Insertion 1 Irradiation Summary Report. 2012. Available: https://www.osti.gov/servlets/purl/1083246 (accessed on 13 August 2025).

[79] Perez DM, Lillo MA, Chang GS, Roth GA, Woolstenhulme NE, *et al.* RERTR-7 Irradiation Summary Report. 2011. Available: https://www.osti.gov/servlets/purl/1033909/ (accessed on 13 August 2025).

[80] Perez DM, Nielsen JW, Chang GS, Wachs DM, Roth GA, *et al.* AFIP-6 mark II irradiation summary report. 2012. Available: https://www.osti.gov/servlets/purl/1083245/ (accessed on 13 August 2025).

[81] Jackson GR, Smith K, Fisher T, McCarthy PT. Simulation of thermal storage in wax-impregnated porous foams with a pore-scale submodel. In 11th AIAA/ASME Joint Thermophysics and Heat Transfer Conference, Atlanta, USA, June 16–20, 2014, p. 3122.

[82] Lawal ZK, Yassin H, Lai DTC, Che Idris A. Physics-informed neural network (PINN) evolution and beyond: a systematic literature review and bibliometric analysis. *Big Data Cogn. Comput.* 2022, 6(4):140.

[83] Navab N, Hornegger J, Wells WM, Frangi A. Medical image computing and computer-assisted intervention–MICCAI 2015. In *18th International Conference*, Munich, Germany, October 5–9, 2015.

[84] Abbott EC, Brenkmann A, Galbraith C, Ong J, Schwerdt IJ, *et al.* Dependence of UO2 surface morphology on processing history within a single synthetic route. *Radiochim. Acta* 2019, 107(12):1121–1131.

[85] Qassim H, Verma A, Feinzimer D. Compressed residual-VGG16 CNN model for big data places image recognition. In *2018 IEEE 8th annual computing and communication workshop and conference (CCWC)*, Las Vegas, USA, January 8–10, 2018, pp. 169–175.

[86] Koo YH, Oh JY, Lee BH, Tahk YW, Song KW. Artificial neural network modeling for fission gas release in LWR UO2 fuel under RIA conditions. *J. Nucl. Mater.* 2010, 405(1):33–43.

[87] Yegnanarayana B. Artificial neural networks, 1st ed. Delhi: PHI Learning Pvt. Ltd., 2009.

[88] Hearst MA, Dumais ST, Osuna E, J Platt, Scholkopf B. Support vector machines. *IEEE Intell. Syst.* 1998, 13(4):18–28.

[89] Sun D, Han F, Ying W. The experimental investigation of water jet–guided laser cutting of CFRP. *Int. J. Adv. Manuf. Technol.* 2019, 102(1):719–729.

[90] Gao M, Yuan S, Wei J, Niu J, Zhang Z, *et al.* Optimization of processing parameters for waterjet-guided laser machining of SiC/SiC composites. *J. Intell. Manuf.* 2024, 35(8):4137–4157.

[91] Zhang D, Liu Y, Liu H, Feng Y, Guo H, *et al.* Characterisation of damage evolution in plain weave SiC/SiC composites using *in situ* X-ray micro-computed tomography. *Compos. Struct.* 2021, 275:114447.

[92] Patel DK, Parthasarathy T, Przybyla C. Predicting the effects of microstructure on matrix crack initiation in fiber reinforced ceramic matrix composites via machine learning. *Compos. Struct.* 2020, 236:111702.

[93] Nasiri A, Bao J, Mccleeary D, Louis SYM, Huang X, *et al.* Online damage monitoring of SiC_f-SiC_m composite materials using acoustic emission and deep learning. *IEEE Access* 2019, 7:140534–140541.

[94] Chao Z, Xiao M, Luan X. Investigation of machine learning methods for oxidation and tensile creep properties of SiC/SiC composites. In *2022 2nd Asia-Pacific Conference on Communications Technology and Computer Science (ACCTCS)*, Shenyang, China, February 25–27, 2022, pp. 247–251.

[95] Wythoff BJ. Backpropagation neural networks: a tutorial. *Chemom. Intell. Lab. Syst.* 1993, 18(2):115–155.

[96] Fu Y, Frazier WE, Choi KS, Li L, Xu Z, *et al.* Prediction of grain structure after thermomechanical processing of U-10Mo alloy using sensitivity analysis and machine learning surrogate model. *Sci. Rep.* 2022, 12(1):10917.

[97] Frazier W, Wang C, Xu Z, Overman N, Hu S, *et al*. Recrystallization and grain growth simulations for multiple-pass rolling and annealing of U-10Mo. *Metall. Mater. Trans. A* 2020, 51:533–544.

[98] Frazier WE, Hu S, Overman N, Lavender C, Joshi VV. Short communication on Kinetics of grain growth and particle pinning in U-10 wt.% Mo. *J. Nucl. Mater.* 2018, 498:254–258.

[99] Yan B, Gao R, Liu P, Zhang P, Cheng L. Optimization of thermal conductivity of UO2–Mo composite with continuous Mo channel based on finite element method and machine learning. *Int. J. Heat Mass Transfer* 2020, 159:120067.

[100] Ye J, Chow JH, Chen J, Zheng Z. Stochastic gradient boosted distributed decision trees. In *Proceedings of the 18th ACM conference on Information and knowledge management*, HK, China, November 2–6, 2009, pp. 2061–2064.

[101] Yan B, Cheng L, Li B, Liu P, Wang X, *et al*. Bi-directional prediction of structural characteristics and effective thermal conductivities of composite fuels through learning from finite element simulation results. *Mater. Des.* 2020, 189:108483.

[102] He K, Zhang X, Ren S, Sun J. Deep residual learning for image recognition. *arXiv* 2015, arXiv:1512.03385.

[103] Dong Y, Lv J, Peng T, Zuo H, Li Q. Predicting the particle-agglomeration effect on the equivalent mechanical properties of dispersion nuclear fuel by machine learning. *J. Nucl. Mater.* 2023, 586:154697.

[104] Zikry MA, Kao M. Inelastic microstructural failure mechanisms in crystalline materials with high angle grain boundaries. *J. Mech. Phys. Solids* 1996, 44(11):1765–1798.

[105] Shanthraj P, Zikry MA. Dislocation density evolution and interactions in crystalline materials. *Acta Mater.* 2011, 59(20):7695–7702.

[106] Hasan T, Capolungo L, Zikry M. A machine learning microstructurally predictive framework for the failure of hydrided zirconium alloys. *npj Mater. Degrad.* 2023, 7(1):22.